

## **A Kinetic Model for Droplet Growth in the Transition Regime**

**G. F. Hubmer<sup>1,2</sup> and U. M. Titulaer<sup>1</sup>**

*Received July 2, 1990; final November 28, 1990*

---

A variant of the moment expansion method, used in an earlier paper to describe the flow of a gas toward an absorbing sphere, is applied to a more realistic model of a droplet condensing from a supersaturated vapor. In the simplest version a spherical droplet absorbs all incoming vapor molecules, but spontaneously emits molecules with a Maxwellian distribution at the droplet temperature and with the corresponding saturated vapor density. From a solution of the stationary linearized Boltzmann equation with these boundary conditions we obtain expressions for the heat and mass currents toward the sphere as a function of the supersaturation and the temperature difference between the droplet and the vapor at infinity. For small droplet radii the known free flow limit is obtained in a natural way. From the calculated expressions for the heat and mass current we derive evolution equations for the radius and temperature of the droplet. The temperature evolves more rapidly and can thus be eliminated adiabatically; the resulting growth curve for the radius shows a sharp transition from a kinetically controlled regime for small radii to a regime dominated by heat conduction for large radii. The effect of incomplete absorption at the surface is also studied. The actual calculations are carried out for Maxwell molecules, with parameters corresponding to argon at  $0.65T_c$  and 100% supersaturation.

---

**KEY WORDS:** Boltzmann equation; droplet growth; moment expansion; kinetic boundary layer; heat and mass transport.

### **1. INTRODUCTION AND SURVEY**

This paper treats a model for the growth of small droplets from a supersaturated vapor. The droplets are assumed to be large compared to the critical radius for nucleation, but not necessarily large on the scale of a

---

<sup>1</sup> Institut für Theoretische Physik, Johannes Kepler Universität Linz, A-4040 Linz, Austria.

<sup>2</sup> Present address: VOEST-ALPINE Industrieanlagenbau GmbH, A-4031 Linz, Austria.

mean free path in the vapor. Such a regime occurs only well below the critical temperature; we shall therefore assume that the density of the liquid is much larger than that of the gas, and that the droplet stays spherical and is always essentially in local equilibrium. As long as the droplet is much smaller than a mean free path, the vapor may be in local equilibrium as well, though possibly at a different temperature. The theory of droplet growth is then straightforward once the boundary conditions for vapor molecules at the droplet surface are known; this regime is known as the free flow regime.<sup>(1,2)</sup> Once the droplet size becomes comparable with the mean free path, a kinetic boundary layer develops around the droplet, and the transport in the vapor depends sensitively on the structure of this layer. In this so-called transition or Knudsen regime no really satisfactory theory of droplet growth exists.<sup>(1,2)</sup> For droplets large compared to a mean free path the boundary layer becomes less important; in this hydrodynamic regime the growth process can be treated using the Navier–Stokes equations.

In a previous paper,<sup>(3)</sup> henceforth denoted by I, we developed a solution procedure for the linearized Boltzmann equation around a totally absorbing sphere that spans the transition regime and connects to known results for the hydrodynamic and free flow regimes, at least for a gas of Maxwell molecules. Since then the method was shown<sup>(4)</sup> to be equally successful for two simple models of a vapor mixed with an inert carrier gas. In the present paper we shall again treat Maxwell molecules, but replace the unrealistic model of a completely absorbing droplet with more realistic boundary conditions at the surface. In particular, we take account of the spontaneous evaporation of molecules off the droplet.

In Section 2 we give a short recapitulation of the formalism of I; since the formalism is used essentially as in I, we refer to that paper for a more detailed explanation and justification of our method. In Section 3 we introduce the model of a *black droplet*, the analog for our problem of a black body in the theory of radiation. Such a droplet absorbs all vapor molecules impinging on it, but in addition emits molecules with a Maxwellian velocity distribution at the droplet temperature and with a density equal to the saturation density at that temperature. From the solution of the stationary linearized Boltzmann equation with these boundary conditions we obtain the particle and heat currents toward the droplet as functions of the temperature difference between the droplet and the vapor at infinity and of the degree of supersaturation. For small values of these driving forces, we obtain a set of Onsager coefficients connecting currents and forces of the type found by Lang<sup>(5)</sup> in a theory that was extended to polyatomic gases, but treated boundary layer effects only approximately.

If we assume that the kinetic energy and the heat of condensation of the arriving particles are distributed instantaneously over the droplet, the expressions found in Section 3 lead to evolution equations for the radius and temperature of the droplet. These equations are given in Section 4 and solved numerically for parameter values corresponding to argon at  $T_0 = 0.65T_c$  and 100% supersaturation. We find that the droplet temperature evolves much faster than the radius; thus this temperature may be eliminated adiabatically from the coupled evolution equations, and we obtain a universal growth curve for the radius. This curve bends over from a roughly linear time dependence of the radius for small radii to a square root dependence at large radii. Moreover, the quasistationary value of the droplet temperature lies about 8% above the vapor temperature at infinity, and the vapor pressure is approximately uniform for not too small radii; this justifies *a posteriori* the use of the *linearized* Boltzmann equation.

The transition from a linear to a square root growth law is typical for the transition from a kinetically-controlled to a diffusion-controlled regime<sup>(1,2,6)</sup> (the relevant process for large radii is *heat diffusion* in our case). To check this interpretation we consider in Section 5 the case of a gray droplet, i.e., of a droplet with sticking and evaporation coefficients less than unity. As expected, the growth rate is proportional to the sticking coefficient for small radii, but becomes virtually independent of the sticking coefficient (as long as it is not extremely small) in the presumed diffusion-controlled regime. The final section contains a few concluding remarks, in particular on the limitations of the model, on its relevance for the design and interpretation of experiments, and on justifications for the approximations made.

The method described in this paper enables one to calculate the growth curve for a droplet when the mesoscopic boundary conditions are known. In practice, the latter are not known very reliably; therefore, the main practical importance of our work is that it provides a way to extract information about mesoscopic boundary conditions from experiments on droplet growth.<sup>(1,2,15)</sup> Before our theory can be used in such a way, a number of effects must be incorporated, as discussed more fully in Section 6; in particular, the theory must be extended to mixtures. On the other hand, the theory becomes rather cumbersome for mixtures of polyatomic gases; it would therefore be very desirable to have accurate experiments on condensation of droplets from gas mixtures in which at least the major component (responsible for the heat transport) is a noble gas.

## 2. THE BASIC EQUATIONS AND THEIR SOLUTION SCHEME

As in I, the main technical task is to solve the stationary linearized Boltzmann equation for Maxwell molecules in the space outside of a sphere, for given boundary conditions at the surface of the sphere. This solution should approach a given equilibrium solution far away from the sphere. We write the distribution function  $f(\mathbf{v}, \mathbf{r})$  for velocity and position of the vapor molecules as

$$f(\mathbf{v}, \mathbf{r}) = n_0 f_M(v; T_0) [1 + \Phi(\mathbf{v}, \mathbf{r})] \quad (2.1)$$

with  $n_0$  and  $T_0$  the density and temperature for  $r \rightarrow \infty$  and  $f_M(v; T_0)$  the Maxwell distribution at  $T_0$ . For spherically symmetric problems  $\Phi$  can be written as

$$\Phi(\mathbf{v}, \mathbf{r}) = \Phi(v, \mu, r); \quad \mu = \hat{\mathbf{v}} \cdot \hat{\mathbf{r}} \quad (2.2)$$

In units such that lengths are measured in mean free paths and velocities in mean thermal velocities [see (I.2.4) for precise definitions],  $\Phi$  must obey the equation

$$v \left( \mu \frac{\partial}{\partial r} + \frac{1 - \mu^2}{r} \frac{\partial}{\partial \mu} \right) \Phi(v, \mu, r) = \beta \eta \mathcal{R}_0 \Phi \quad (2.3)$$

where  $\eta$  is the shear viscosity,  $\beta$  equals  $(kT_0)^{-1}$ , and  $\mathcal{R}_0$  is the linearized Boltzmann operator. The partial differential equation (2.3) may be transformed into a set of coupled ordinary differential equations by the substitution

$$\Phi(v, \mu, r) = \sum_{n,k} A_{nk}(r) \psi_{nk}(v, \mu) \quad (2.4)$$

where the  $\psi_{nk}$  ( $n, k = 0, 1, 2, \dots$ ) are the Burnett functions.<sup>(3,7)</sup> The Burnett functions are eigenfunctions of  $\mathcal{R}_0$ , with eigenvalues of order  $(\beta\eta)^{-1}$ , for the special case of Maxwell molecules.

We now look for special solutions of the form

$$A_{nk}(r) = a_{nk}^{(q)} \left( \frac{2}{\pi q r} \right)^{1/2} K_{k+1/2}(qr) \quad (2.5)$$

where  $K_\nu(r)$  denotes the modified Bessel function, which decays for large  $r$  as  $r^{-1/2} e^{-r}$ . Substitution of (2.4) and (2.5) into (2.3) leads to a generalized eigenvalue problem of the type

$$q \mathbf{B} \cdot \mathbf{a}^{(q)} = \mathbf{A} \cdot \mathbf{a}^{(q)} \quad (2.6)$$

where  $\mathbf{a}^{(q)}$  is a vector containing the coefficients  $a_{nk}^{(q)}$  and  $\mathbf{B}$  and  $\mathbf{A}$  are infinite matrices representing the action of the operators on the two sides of (2.3). In particular,  $\mathbf{A}$  is diagonal for Maxwell molecules; for further details we refer to I. The (degenerate)  $q=0$  sector of the eigenvalue problem (2.6) needs separate treatment. One finds<sup>(3,8)</sup> two eigenfunctions  $\Phi_p$  and  $\Phi_h$ , corresponding to a uniform increase in density and temperature, and two associated eigenfunctions  $\Phi_{pc}$  and  $\Phi_{hc}$  corresponding to particle and heat currents. The latter solutions have  $A_{nk}(r)$  obeying

$$A_{nk}(r) = a_{nk}^{(0,i)} g_k(r); \quad g_0(r) = \frac{1}{r}; \quad g_k(r) = \frac{(2k-1)!!}{r^{k+1}} \quad (2.7)$$

Our further developments are based on the half range completeness conjecture (see I for further details), which states that solutions with  $\Phi$  vanishing at  $r \rightarrow \infty$  and given spherically symmetric boundary conditions at  $r = R$  can be written *uniquely* in the form

$$\Phi(v, \mu, r; R) = C(R)\Phi_{pc} + D(R)\Phi_{hc} + \sum_i d_i(R)\Phi_i^{(+)} \quad (2.8)$$

where the  $\Phi_i^{(\pm)}$  are the special solutions derived from solutions of (2.6) with positive eigenvalues  $q_i$ . In practice, (2.6) cannot be solved in closed form; approximate numerical solutions are obtained by truncating the expansion (2.4). We shall use the truncation prescriptions, applied successfully in I,

$$D_N: \quad a_{nk}^{(q)} = 0 \quad \text{for } n+k > N; \quad a_{N0}^{(q)} = 0 \quad (2.9)$$

This series of truncations contains Grad's 13-moment approximation<sup>(9)</sup> as  $D_2$ . Explicit solutions are obtained by truncating  $\Phi_{pc}$  and  $\Phi_{hc}$  accordingly, restricting the sum in (2.8) to  $\Phi_i^{(\pm)}$  with finite  $q_i^{-1}$ , and replacing the exact boundary condition

$$f(v, \mu, R; R) = g(v, \mu) \quad \text{for } \mu > 0 \quad (2.10a)$$

by its Marshak-type analog<sup>(10)</sup>

$$\int_0^1 d\mu \int_0^\infty v^2 dv [f(v, \mu, R; R) - g(v, \mu)] \psi_{n,2k+1}(v, \mu) = 0 \quad (2.10b)$$

for all  $n, k$  with  $n+2k < N$ . This provides precisely the number of conditions required to make the truncated version of (2.8) unique, as was shown in I.

### 3. THE SOLUTION FOR A "BLACK" DROPLET

In I we solved the mathematically simple, but physically unrealistic case  $g(v, \mu) = 0$ , corresponding to complete absorption of all impinging vapor molecules without any reemission. In the present paper we include spontaneous evaporation off the droplet. If we maintain the requirement of complete absorption (perfect sticking) and assume that the distribution of spontaneously emitted particles does not depend on the state of the vapor, then the requirement that detailed balance holds in the special case of a vapor at saturation density  $n_s(T_D)$ , with  $T_D$  the droplet temperature, leads to the requirement

$$g(v, \mu) = n_s(T_D) f_M(v; T_D) \quad (3.1)$$

with  $f_M$  the Maxwell distribution at temperature  $T_D$ .

The boundary problem sketched above was solved for various  $R$  in various approximations  $D_N$ . Physically, the most interesting aspects of the solution are the resulting particle and (modified) heat current densities

$$\mathbf{J}_p(r) = \int d\mathbf{v} \mathbf{v} f(v, r) \sim \int d\mathbf{v} \psi_{01}(v, \mu) f(v, \mu, r) \quad (3.2a)$$

$$\mathbf{J}_h(r) = \int d\mathbf{v} \mathbf{v} \left[ \frac{v^2}{2} - \frac{5}{2} \right] f(v, \mu, r) \sim \int d\mathbf{v} \psi_{11}(v, \mu) f(v, \mu, r) \quad (3.2b)$$

From (2.8) and the specific form of the special solutions contained in it<sup>(3)</sup> one sees that  $\mathbf{J}_p$  and  $\mathbf{J}_h$  are proportional to  $C(R)$  and  $D(R)$  respectively [the  $\Phi_i^{(+)}$  have no (01) and (11) components]; moreover, one sees from (2.7) that they depend on  $r$  like  $r^{-2}$  (which also follows from particle and energy conservation in the Boltzmann equation).

For  $T_D$  and  $n_s(T_D)$  close to  $T_0$  and  $n_0$ , the currents  $\mathbf{J}_p$  and  $\mathbf{J}_h$  become linear in the differences. In analogy to ref. 5, we use as our variables

$$\frac{\Delta T}{T_0} = \frac{T_D - T_0}{T_0}, \quad \frac{\Delta p}{p_0} = \frac{n_s(T_D) - n_0}{n_0} + \frac{\Delta T}{T_0} \quad (3.3)$$

where we used the (linearized) ideal gas law, and write the resulting  $\mathbf{J}_p$  and  $\mathbf{J}_h$  in the form familiar from irreversible thermodynamics:<sup>(5)</sup>

$$\mathbf{J}_p = \mathbf{J}_0 \frac{R^2}{r^2} \left[ \alpha_{pp} \frac{\Delta p}{p_0} + \alpha_{ph} \frac{\Delta T}{T_0} \right] \quad (3.4a)$$

$$\mathbf{J}_h = \mathbf{J}_0 \frac{R^2}{r^2} \left[ \alpha_{hp} \frac{\Delta p}{p_0} + \alpha_{hh} \frac{\Delta T}{T_0} \right] \quad (3.4b)$$

with

$$\mathbf{J}_0 = \hat{\mathbf{e}}_r n_0 (2\pi m \beta)^{-1/2} \quad (3.4c)$$

The results obtained for the Onsager coefficients  $\alpha_{ij}$  are given in Fig. 1 for the  $D_2$  (13-moment) and  $D_8$  approximations. We shall not go beyond the  $D_8$  approximation in this paper, since we saw in I that higher  $D_N$  provide only slight improvements. The exactly known results in the free flow limit [ $R \downarrow 0$ ,  $\Phi(v, \mu) \rightarrow 0$ ], namely  $\alpha_{pp} = 1$ ,  $\alpha_{hh} = 9/4$ ,  $\alpha_{hp} = -1/2$ , are indicated by arrows. We see that the  $D_2$  results are off in this limit by factors of order unity; the  $D_8$  results are close to their free flow values at the  $R$  values where they break down due to the numerical inaccuracies associated with the singularities in the expressions (2.7) and the comparable singularities in the  $K_{k+1/2}(qr)$ . Down to this point of breakdown, the Onsager relation  $\alpha_{ph}(R) = \alpha_{hp}(R)$  is also satisfied up to the numerical uncertainty.

The function  $\alpha_{pp}(R)$  is identical with the normalized reaction rate  $\hat{k}(R)$  for a completely absorbing sphere, shown in Fig. 1b of I. This follows from the fact that our present boundary condition (2.10a), with  $g(v, \mu)$  given by (3.1), is fulfilled for the special case  $T_D = T_0$  by

$$f(v, \mu, r) = f_M(v; T_0) \{ n_s + (n_0 - n_s) [1 + \Phi_a(v, \mu, r; R)] \} \quad (3.5)$$

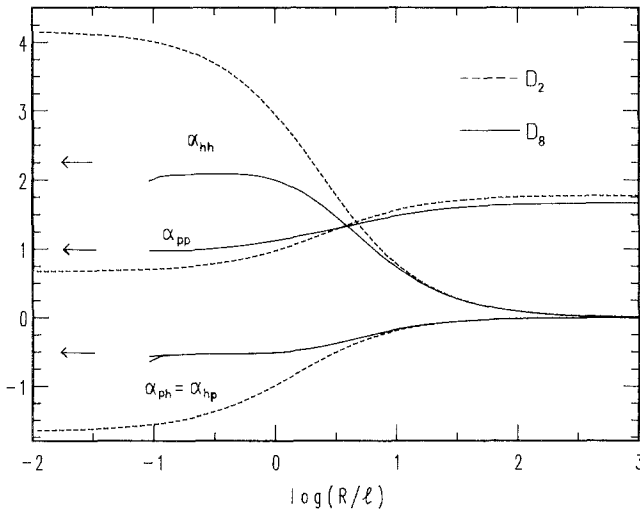


Fig. 1. The Onsager coefficients defined in (3.4) as functions of  $\log R$  (in units of the mean free path  $l$ ) in the  $D_2$  and  $D_8$  approximations. The arrows denote the known  $R \downarrow 0$  limits.

where  $\Phi_a$  is the solution with  $g(\mathbf{v})=0$ , studied in I. Finally we note that, whereas  $\alpha_{pp}$  remains of order unity for  $R \rightarrow \infty$ , the other Onsager coefficients decrease like  $R^{-1}$  in that limit; this reflects the fact that heat transport becomes diffusive for large  $R$  ( $\mathbf{J}_h \sim RAT/r^2$ );  $\alpha_{hp}$  and  $\alpha_{ph}$  must then also become of order  $R^{-1}$  to keep the Onsager matrix positive definite.

Our treatment differs from the one in ref. 5 (and earlier ones quoted there) in a number of respects. The earlier treatments take into account only those moments treated in our  $D_2$  approximation, to which they reduce for  $R \rightarrow \infty$ ; thus, genuine boundary layer effects are not included, and their inclusion would require major modifications. The correct behavior for  $R \downarrow 0$  is enforced by replacing the expansion (2.4) by separate Maxwellians, with different density profiles and temperatures, for particles with velocities pointing away from the droplet and all other particles. Thus, the approach to the correct  $R \downarrow 0$  limit no longer serves as a check on the theory. Further comments on the relation of our treatment to that of ref. 5 are given elsewhere.<sup>(11)</sup>

#### 4. THE GROWTH OF A BLACK DROPLET

From the solution (3.4) of the stationary linearized Boltzmann equation one may derive evolution equations for the droplet radius  $R$  and the droplet temperature  $T_D$  by assuming that the heat of condensation released by the arriving particles and their kinetic energy are distributed instantaneously over the droplet, and that the droplet stays spherical in shape. The use of *stationary* solutions must be checked afterward. It can be justified only if  $R$  and  $T_D$  change slowly on the time scale of typical relaxation times in the gas; in particular, the growth velocity of the droplet should be small compared with the thermal velocity. To facilitate the interpretation of our expressions we return to regular units for the first part of the present section.

The quantities needed from the solution of the Boltzmann equation are the total particle current

$$4\pi R^2 |\mathbf{J}_p| \equiv n_0 k(R, T_D) = n_0 \kappa_p(R, T_D) k_{\text{kin}}(R) \quad (4.1)$$

where  $k_{\text{kin}}(R)$  is the free flow ( $R \downarrow 0$ ) value for the reaction coefficient  $k(R)$ ,

$$k_{\text{kin}}(R) = 4\pi R^2 (2\pi m\beta)^{-1/2} \quad (4.2)$$

and the flow of kinetic energy [cf. (3.2)]

$$4\pi R^2 \left| \mathbf{J}_h + \frac{5}{2\beta} \mathbf{J}_p \right| \equiv n_0 \beta^{-1} \kappa_h(R, T_D) k_{\text{kin}}(R) \quad (4.3)$$



For the change in the droplet volume  $V_D$  we obtain

$$\frac{d}{dt} V_D = \frac{n_0}{n_l(T_D)} k(R, T_D) + \alpha_p V_D \frac{d}{dt} T_D \quad (4.4)$$

where  $n_l(T_D)$  denotes the liquid density at  $T_D$  and  $\alpha_p$  the thermal expansion coefficient. Similarly we find for the change in the heat content  $Q_D$  of the droplet

$$\frac{d}{dt} Q_D = n_0 k_{\text{kin}}(R) \left[ \frac{\kappa_h(R, T_D)}{\beta} - \frac{3\kappa_p(R, T_D) T_D}{2\beta T_0} + \kappa_p(R, T_D) \Delta\tilde{h} \right] \quad (4.5)$$

where  $\Delta\tilde{h}$  denotes the heat of condensation per particle (the definition of  $\Delta\tilde{h}$  assumes that a vapor molecule entering the liquid carries the thermal energy  $3k_B T_D/2$ ).

Next we transform (4.4) into an equation for the droplet radius:

$$\frac{dR}{dt} = \frac{n_0}{n_l(T_D)} (2\pi m\beta)^{-1/2} \kappa_p(R, T_D) + \frac{\alpha_p R}{3} \frac{dT_D}{dt} \quad (4.6)$$

Similarly we obtain from (4.5) an equation for  $T_D$  by dividing by the heat capacity of the droplet and correcting for the volume change; this leads to

$$V_D \frac{dT_D}{dt} = \frac{N_A}{C_p(T_D) n_l(T_D)} \frac{dQ}{dt} - T_D \frac{dV_D}{dt} \quad (4.7)$$

where  $N_A$  is Avogadro's number and  $C_p$  is the heat capacity per mole at constant pressure (which is virtually equal to the heat capacity along the coexistence curve).

For our further calculations we introduce dimensionless quantities  $\hat{R}$ ,  $\hat{T}$ , and  $\hat{t}$ :

$$R = l\hat{R}, \quad T_D = T_0\hat{T}, \quad t = \frac{\eta\beta}{n_0} \frac{n_l(T_0)}{n_s(T_0)} \hat{t} \quad (4.8)$$

where  $n_s(T)$  again denotes the density of the saturated vapor at  $T$ ; the combination  $t_c = \eta\beta/n_0$  is the mean free time between collisions in the vapor. If we further eliminate  $n_0$  in favor of the supersaturation parameter

$$\sigma = n_0 [n_s(T_0)]^{-1} \quad (4.9)$$

and the condensation energy per particle  $\Delta\tilde{h}$  in favor of the corresponding energy per mole  $\Delta h$ , we obtain after a few trivial rearrangements

$$\frac{d\hat{R}}{d\hat{t}} = \frac{\sigma}{(2\pi)^{1/2}} \frac{n_l(T_0)}{n_l(\hat{T}T_0)} \kappa_p(\hat{R}, \hat{T}) + \frac{\alpha_p T_0}{3} \hat{R} \frac{d\hat{T}}{d\hat{t}} \quad (4.10a)$$

$$\frac{d\hat{T}}{d\hat{t}} = \frac{3\sigma n_l(T_0)}{\hat{R} n_l(\hat{T}T_0)} \frac{1}{1 + \alpha_p \hat{T}T_0} \frac{\mathcal{R}}{C_p} \left\{ \kappa_h(\hat{R}, \hat{T}) + \frac{\kappa_p(\hat{R}, \hat{T})}{(2\pi)^{1/2}} \right. \\ \left. \times \left( \frac{\Delta h}{\mathcal{R}T_0} - \frac{3\hat{T}}{2} - \frac{\hat{T}C_p}{\mathcal{R}} \right) \right\} \quad (4.10b)$$

where  $\mathcal{R}$  denotes the gas constant.

We solved this set of equations numerically in  $D_2$  and  $D_8$  approximation for parameters<sup>(12)</sup> corresponding to argon with  $T_0 = 0.65T_c$  and  $\sigma = 2$ . For  $n_s(T)$  and  $n_l(T)$  we used the universal equation of state<sup>(13)</sup>

$$n_{l,s}(T) = n_c \left[ 1 + \frac{3}{4} \left( 1 - \frac{T}{T_c} \right) \pm \frac{7}{4} \left( 1 - \frac{T}{T_c} \right)^{1/3} \right] \quad (4.11)$$

where  $T_c$  and  $n_c$  are the critical temperature and density, respectively. A typical result for  $\hat{R}(\hat{t})$  in the  $D_8$  approximation, with  $\hat{R}(0) = 10$  and several values of  $\hat{T}(0)$ , is shown in Fig. 2; the qualitative behavior for smaller  $\hat{R}(0)$  is similar. One sees that the initial growth rates for different  $\hat{T}(0)$  differ appreciably, but the curves become parallel after the rapid transient. The corresponding curves for  $\hat{T}(\hat{t})$  converge on the same time scale to a "working temperature"  $\hat{T}_w(\hat{R})$ , which, to a very good approximation, is the

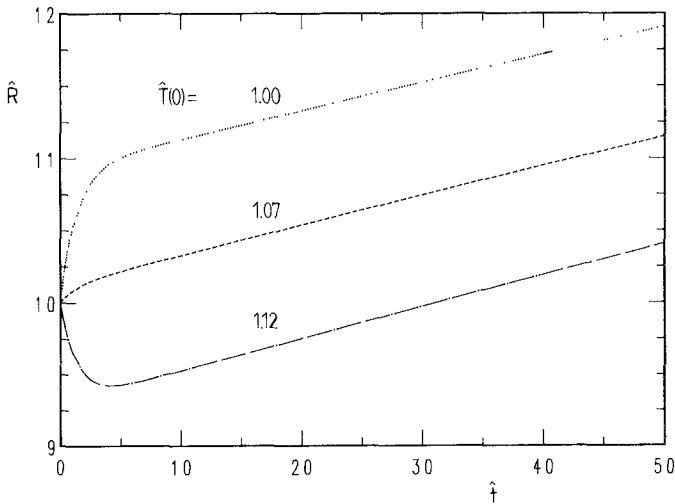


Fig. 2. The solution  $\hat{R}(\hat{t})$  obtained from (4.10) for  $\hat{R}(0) = 10$  and various values of  $\hat{T}(0)$  in the  $D_8$  approximation. The units are specified in (4.8); the parameters used correspond to argon at  $0.65T_c$  and 100% supersaturation.

temperature at which the expression in (4.10b) for  $d\hat{T}/d\hat{t}$  vanishes. For large  $\hat{R}$  the function  $T_w(\hat{R})$  has the form

$$\begin{aligned} \hat{T}_w(\hat{R}) &\simeq 1.078727\dots - 0.012\dots \hat{R}^{-1} && \text{for } D_2 \\ \hat{T}_w(\hat{R}) &\simeq 1.078779\dots - 0.014\dots \hat{R}^{-1} && \text{for } D_8 \end{aligned} \tag{4.12}$$

Both values for  $\hat{T}_w(\infty)$  in (4.12) lie very close to the isobaric temperature  $T_i$  defined by

$$p_s(T_i) = p_0, \quad \text{or} \quad n_s(T_i)T_i = n_0T_0 \tag{4.13}$$

which for our choice of parameters is given by  $\hat{T}_i = 1.078821\dots$ . [The small discrepancy, which persists in higher  $D_N$  approximations, is probably due to corrections to (3.4a) of higher order in  $\Delta T$ .] At the droplet temperature  $T_i$  the pressure difference  $\Delta p$  in (3.4) vanishes, and the droplet growth is dominated by  $\alpha_{ph}$ , which, as we saw, is of order  $\hat{R}^{-1}$  relative to  $\alpha_{pp}$ . Thus, one expects that  $\kappa_p[\hat{R}, T_w(\hat{R})]$  is of order  $\hat{R}^{-1}$  throughout the region where  $T_w(\hat{R}) - T_i$  is of order  $\hat{R}^{-1}$ .

This expectation is borne out by the numerical solution  $\hat{R}(\hat{t})$  of (4.6), with  $T = T_w(\hat{R})$  and the second term omitted, presented in Fig. 3 on a doubly logarithmic scale. Especially in the  $D_8$  approximation (supplemented by an interpolation to the known  $R \downarrow 0$  limit for values of  $\hat{R}$

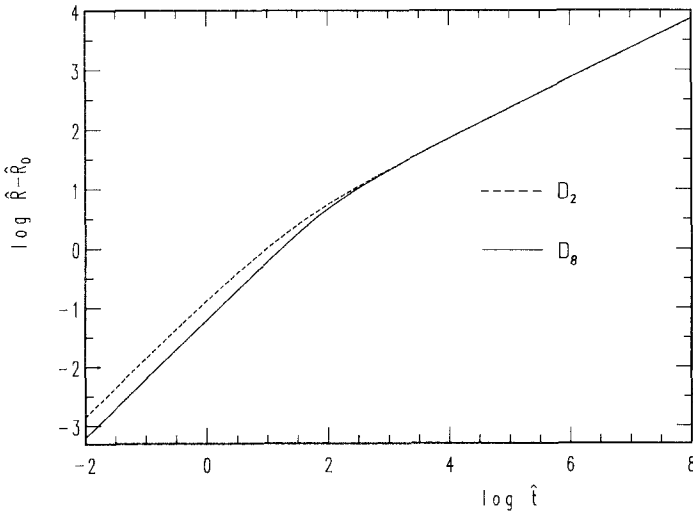


Fig. 3. The growth curve  $\hat{R}(\hat{t})$  obtained from (4.10) after adiabatic elimination of the temperature, in  $D_2$  and  $D_8$  approximations, plotted on a doubly logarithmic scale. Parameters and units as in Fig. 2.

where  $D_8$  breaks down) we find a rather sharp transition between a low- $\hat{R}$  regime  $\hat{R}(\hat{i}) \sim \hat{i} - \hat{i}_0$ , corresponding to  $d\hat{R}/d\hat{i} = \mathcal{O}(1)$ , and a high- $\hat{R}$  regime  $\hat{R}(\hat{i}) \sim (\hat{i} - \hat{i}_0)^{1/2}$ , corresponding to  $d\hat{R}/d\hat{i} = \mathcal{O}(\hat{R}^{-1})$ . These time dependences are characteristic for kinetically and diffusion-controlled processes respectively. The relevant diffusion process is heat conduction; the rate of condensation is limited by the amount of heat that can be carried away to infinity once the droplet temperature has reached a value close to  $\hat{T}_w(\infty)$ . From Fig. 2 one also sees that the influence of the kinetic boundary layer, responsible for the difference between  $D_2$  and  $D_8$ , is large for small  $\hat{R}$ , in accordance with the trends shown in Fig. 1 for the fully linearized theory. For large  $\hat{R}$  some differences between  $D_2$  and  $D_8$  persist; they are barely visible in the figure, but are seen in singly logarithmic plots.<sup>(8)</sup>

## 5. THE GROWTH OF "GRAY" DROPLETS

The physical picture emerging at the end of the preceding section can be checked by considering a droplet that reflects some of the vapor molecules hitting it (with a corresponding reduction of the spontaneous evaporation rate). If the above picture is correct, then for  $\hat{R} \downarrow 0$ , where the presence of the droplet hardly influences the particle distribution in the surrounding vapor, the growth rate should be proportional to the sticking coefficient, defined as the fraction of incoming particles that is absorbed. For large droplets, the droplet temperature should approach the isobaric temperature  $T_i$ , irrespective of details of the processes at the surface. The growth rate is then limited by the amount of heat that can be carried off, and hence independent of the sticking coefficient. The same prediction follows from probabilistic expectations, guided by the well-known results in the theory of Brownian motion. A particle that arrives from the region of large  $r$  and is reflected by a sphere small compared to  $l$  is very unlikely ever to return there. A particle reflected by a large sphere "sees" the surface as approximately planar and has a high probability, approaching unity for  $R \rightarrow \infty$ , of returning to the surface once more, which gives it another chance of being absorbed.

To test these predictions, and to study details of the transition between the two extremes, we treat a model in which the sticking coefficient  $\alpha$  is independent of velocity, and the molecules not absorbed are reflected specularly. In the notation of (2.10a) such a "gray" droplet is characterized by [cf. also (3.1)]

$$g(v, \mu) = \alpha n_s(T_D) f_M(v; T_D) + (1 - \alpha) f(v, -\mu, R) \quad (5.1)$$

[The sticking and evaporation coefficients should be taken to be equal to

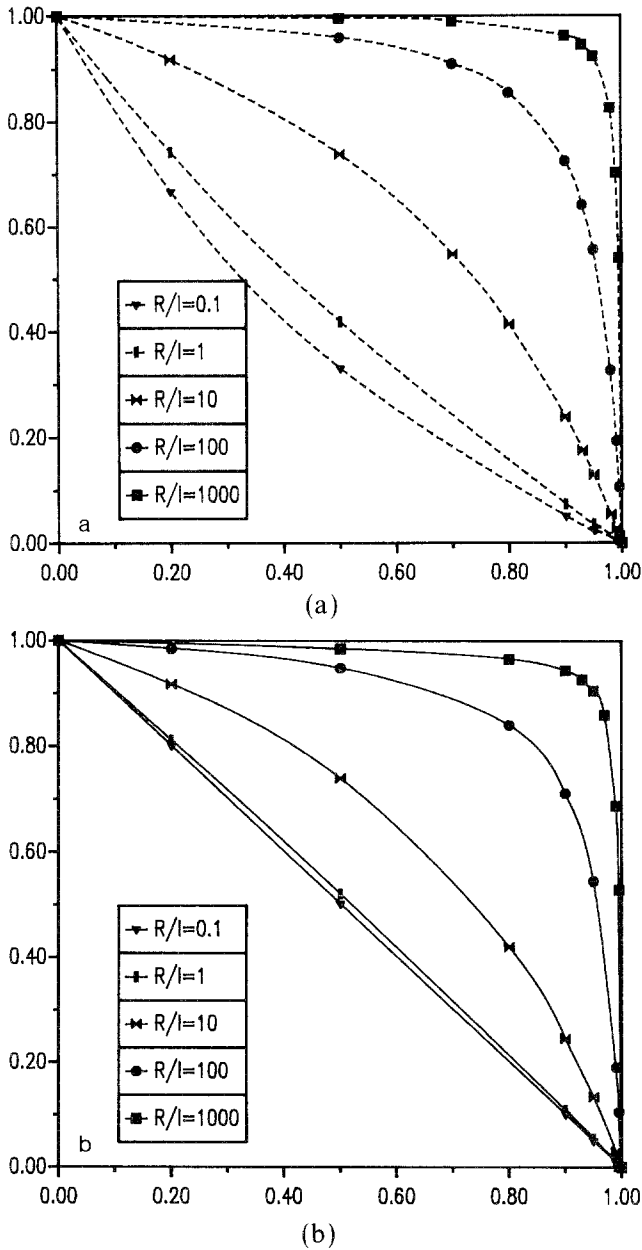


Fig. 4. The growth rate  $d\hat{R}/d\hat{t}$  for a partially absorbing sphere, defined more fully in (5.1), normalized by the rate for a fully absorbing sphere, as a function of the reflection coefficient  $(1-\alpha)$ , as calculated in (a) the  $D_2$  and (b) the  $D_8$  approximations, for various values of  $\hat{R}$ . The symbols denote calculated values; the curves are mere guides to the eye.

preserve detailed balance for vapor temperature  $T_0$  and vapor density  $n_s(T_0)$ ; this is the analog of Kirchhoff's law in the theory of radiation.]

We carried out the program described in Sections 3 and 4 for this boundary condition as well. The results for the growth rate  $d\hat{R}/d\hat{t}$  at the (in general  $\alpha$ -dependent) working temperature  $T_w(\hat{R}; \alpha)$ , normalized by the corresponding quantity at  $\alpha = 1$ , are given for several values of  $\hat{R}$  and  $\alpha$  in Figs. 4a and 4b for the  $D_2$  and  $D_8$  approximations. The results in Fig. 4b are in full agreement with our expectations; in particular we find independence of  $\alpha$ , except for very low  $\alpha$ , at large  $\hat{R}$ . The inadequacy of the  $D_2$  scheme at low  $\hat{R}$ , already evident in Figs. 1 and 3, manifests itself most clearly in the completely unphysical sublinear dependence of  $d\hat{R}/d\hat{t}$  on  $\alpha$  for  $\hat{R} = 0.1$  and  $\hat{R} = 1$  in Fig. 4a. Perhaps more surprising is the quite noticeable discrepancy between  $D_2$  and  $D_8$  for small  $\alpha$ , even at relatively large  $\hat{R}$ . We shall comment on this point in connection with a similar phenomenon in the heat conduction problem in a forthcoming paper.<sup>(14)</sup>

From a practical standpoint, the most important message from Fig. 4b is that a noticeable dependence of the growth rate on  $\alpha$  persists up to rather large values of  $\hat{R}$ . Thus, even experiments in the by now well-accessible (see, e.g., ref. 15) region  $\hat{R} \simeq 10$  could yield useful information about the parameter  $\alpha$ , poorly known in practice, once the theory is adapted to the systems (gas mixtures) for which experiments are performed. It is also clear that experiments on large droplets are of little value in this respect, unless  $\alpha$  turns out to be very small.

## 6. CONCLUDING REMARKS

The understanding of droplet growth in the Knudsen regime was up to now hampered by two problems.<sup>(1,2)</sup> The boundary conditions to be used for the kinetic equations at the liquid-vapor interface (sticking and evaporation coefficients) are poorly known, and there were up to now no reliable methods to solve the kinetic equations for given boundary conditions without arbitrary or uncontrolled approximations. We have shown in this paper that the variant of the moment expansion method developed in I, and applied there to a rather artificial model, is also capable of treating a model that includes most of the relevant physics of the problem. Thus it appears feasible to extract information about the as yet unknown boundary conditions from an analysis of experiments on droplet growth. As we saw in the preceding section, such experiments should be done in the Knudsen region, but radii no smaller than about ten mean free paths would probably be small enough.

Before our model can be used to analyze existing or proposed experiments a number of additional features must be incorporated, notably

the dependence of the saturated vapor density  $n_s(T)$  on the droplet radius due to surface tension effects. Also, one should proceed from Maxwell molecules to more realistic intermolecular interactions, and include the effect of an inert carrier gas. We shall not consider such issues here in more detail; some remarks are given elsewhere.<sup>(11)</sup> We will add a few comments, however, on some of the other crucial simplifying assumptions made in the course of our treatment, and on means to relax some of them.

The most serious restriction lies in our use of the *linearized* Boltzmann equation. As we saw in Section 4, even for a supersaturation of 100%, the density and temperature variations in the quasistationary regime amount to no more than about 10%, so nonlinear effects should not be too important. Still, there is room for some improvement. Outside of the boundary layer our solution of the Boltzmann equation becomes of Chapman–Enskog type. This limiting solution could be replaced by a Chapman–Enskog solution of the full nonlinear Boltzmann equation, with boundary conditions provided by an analysis of the kinetic boundary layer for the linearized equation, as discussed elsewhere (see refs. 6, 14, and 16, especially the last part of Section 3 of the latter). Solutions of the Navier–Stokes equations from which such Chapman–Enskog solutions can be obtained were constructed recently by Luk'yanchuk *et al.*<sup>(17)</sup> for a gas mixture around a heated sphere, with chemical reactions occurring at the surface of the sphere. The state around which one linearizes could then also be chosen more appropriately; one possibility is to choose the isobaric temperature  $T_i$  of (4.13) and the associated density  $n_s(T_i)$ , instead of the values  $T_0$  and  $n_0$  of the vapor at infinity.

The smallness of nonlinear effects in the quasistationary state can also be invoked to justify our slightly inconsistent linearization procedure; we linearized the Boltzmann equation, but not its boundary conditions, except in (3.2) and in the results presented in Fig. 1. This was done mainly for numerical convenience; some checks<sup>(8)</sup> showed that a consistent linearization did not give significantly different results.

An important simplification was obtained by our use of *stationary* solutions to determine the parameters in the evolution equations for  $\hat{R}$  and  $\hat{T}$ . As we pointed out, a necessary condition is that  $dR/dt$  is small compared with the thermal velocity  $(m\beta)^{-1/2}$ . From (4.6) one sees that this is the case once the temperature transients are over. The factor  $n_0/n_i(T_0)$  is equal to 1/42.7 for our choice of parameters, whereas  $\kappa_p(R, T_0)$  is at most of order unity, and usually much smaller: for a fully absorbing sphere  $\kappa_p$  is equal to the parameter  $\alpha_{pp}$  shown in Fig. 1; the spontaneous evaporation included in the present model clearly leads to an appreciable reduction in  $\kappa_p$  relative to the fully absorbing case. The use of stationary solutions becomes somewhat more problematic during the fast transient shown in Fig. 2. In actual

experiments, however, these transients occur already in the nucleation stage, where our model does not yet apply anyhow.

The adiabatic elimination of  $T$  from (4.10a) could also be performed somewhat more carefully<sup>(18)</sup>; one could substitute

$$\frac{d\hat{T}}{d\hat{t}} \cong \frac{d\hat{T}_w(\hat{R})}{d\hat{R}} \frac{d\hat{R}}{d\hat{t}} \quad (6.1)$$

instead of dropping the second term completely. However, this causes only minute corrections in view of the smallness of  $\alpha_p$  and the very weak dependence of  $\hat{T}_w$  on  $\hat{R}$  [cf. (4.12)], except possibly for very small  $\hat{R}$ , where the factor of  $\hat{R}$  reduces the effect.

Finally, we want to stress once more that our treatment makes sense only well away from the critical point. This assumption enters in a number of places. First, we assumed that the droplet reaches equilibrium almost instantaneously on the time scale  $t_0 = t_c n_l/n_s$  that governs the droplet growth. Near the critical point the mean free time in the liquid is comparable with that in the gas, and  $n_l/n_s$  is of order unity; hence the transport of heat to the droplet center requires a time much longer than  $t_0$ . Second, we assumed that the droplet remains spherical, which requires a large surface tension, also absent near the critical point. Third, the small difference between  $\hat{T}_w$  and  $T_0$ , essential to the use of linearized equations, derives from the steepness of the coexistence curve (4.11) at the density  $n_0$ , whereas the rapidity of the transients in Fig. 2, which enabled us to eliminate  $\hat{T}$  adiabatically, is ultimately caused by the large value of the heat of condensation. Both features disappear near  $T_c$ . Our justification for using stationary solutions of the Boltzmann equation in constructing the evolution equation for  $\hat{R}(\hat{t})$  again relied on the fact that  $n_l/n_s$  is large. Finally, the use of the Boltzmann equation itself becomes questionable once the vapor ceases to be dilute. Thus, closer to  $T_c$  one needs a fundamentally different theory, which treats liquid and vapor on a much more equal footing.

## ACKNOWLEDGMENTS

We thank Markus Widder for a number of helpful comments. This work was supported by the Austrian Fonds zur Förderung der wissenschaftlichen Forschung.

## REFERENCES

1. J. C. Barret and C. F. Clement, *J. Aerosol Sci.* **19**:223 (1988).
2. E. J. Davis, *Aerosol Sci. Technol.* **2**:121 (1983).



3. G. F. Hubmer and U. M. Titulaer, *J. Stat. Phys.* **59**:441 (1990).
4. M. E. Widder and U. M. Titulaer, *Physica A* **167**:663 (1990).
5. H. Lang, *Phys. Fluids* **26**:2109 (1983); R. E. Sampson and G. S. Springer, *J. Fluid Mech.* **36**:577 (1969); P. M. Shankar, *J. Fluid Mech.* **40**:385 (1970).
6. M. E. Widder and U. M. Titulaer, *J. Stat. Phys.* **55**:1109 (1989).
7. C. Cercignani, *Theory and Application of the Boltzmann Equation* (Scottish Academic Press, Edinburgh, 1975); *The Boltzmann Equation and Its Applications* (Springer, New York, 1988).
8. G. F. Hubmer, Doctoral Thesis, Linz University (1990).
9. H. Grad, *Commun. Pure Appl. Math.* **2**:331 (1949); **5**:257 (1952).
10. R. E. Marshak, *Phys. Rev.* **71**:443 (1947).
11. G. F. Hubmer and U. M. Titulaer, in *Proceedings of the 17th International Symposium on Rarefied Gas Dynamics, Aachen 1990*, to be published.
12. J. S. Rowlinson, *Liquids and Liquid Mixtures* (Butterworth, London, 1969).
13. E. A. Guggenheim, *J. Chem. Phys.* **13**:253 (1945).
14. G. F. Hubmer and U. M. Titulaer, *Physica A*, to be published.
15. A. Majerowicz and P. E. Wagner, in *Atmospheric Aerosols and Nucleation* (Lecture Notes in Physics 309), P. E. Wagner and G. Vali, eds. (Springer, Berlin, 1988), p. 27.
16. M. E. Widder and U. M. Titulaer, *J. Stat. Phys.* **56**:471 (1989).
17. B. Luk'yanchuk, K. Piglmayer, N. Kirichenko, and D. Bäuerle, *Proceedings of the European Materials Research Society Symposium, Strassbourg 1990*, to be published; D. Bäuerle, B. Luk'yanchuk, and K. Piglmayer, *Appl. Phys. A* **50**:385 (1990).
18. N. G. van Kampen, *Phys. Rep.* **124**:69 (1985).